JOURNAL OF ELECTROMAGNETIC ENGINEERING AND SCIENCE, VOL. 15, NO. 2, 104~110, APR. 2015

http://dx.doi.org/10.5515/JKIEES.2015.15.2.104
ISSN 2234-8395 (Online) · ISSN 2234-8409 (Print)

Magnetic Resonance-Based Wireless Power Transmission through Concrete Structures

Ji-Min Kim[1] · Minseok Han[2,*] · Hoon Sohn[1]

Abstract

As civil infrastructures continue to deteriorate, the demand for structural health monitoring (SHM) has increased. Despite its outstanding capability for damage identification, many conventional SHM techniques are restricted to huge structures because of their wired system for data and power transmission. Although wireless data transmission using radio-frequency techniques has emerged vis-à-vis wireless sensors in SHM, the power supply issue is still unsolved. Normal batteries cannot support civil infrastructure for no longer than a few decades. In this study, we develop a magnetic resonance-based wireless power transmission system, and its performance is validated in three different mediums: air, unreinforced concrete, and reinforced concrete. The effect of concrete and steel rebars is analyzed.

Key Words: Magnetic Resonance, Reinforced Concrete, Structural Health Monitoring, Wireless Power Transmission.

I. Introduction

As the deterioration of civil infrastructure continues, the demand for accurate and efficient structural health monitoring (SHM) techniques has increased rapidly. SHM techniques using various sensors, such as accelerometers, strain sensors, and piezoelectric sensors, have been investigated and their performance has been validated by many studies [1−3]. However, expensive and heavy wiring systems for each type of sensor used to transfer monitoring data and power restricts their use in large civil infrastructures. In recent years, wireless sensors for SHM have attracted significant attention, and notable advancements in wireless data transmission techniques have boosted the refinement of wireless sensors [4, 5]. However, wireless sensors mainly rely on limited battery power, and battery power cannot support wireless sensors for the lifespan of civil infrastructure.

A new powering strategy is necessary to use wireless sensors. As an alternative, researchers have suggested energy harvesting, which can harness energy from the surrounding environment, such as vibrations and natural light [6−8]. Energy harvesting is considered a promising technique to power wireless sensors without human labor after the initial installation. However, the amount of power collected, from a few μW to mW, would not be sufficient to operate wireless sensors. In addition, specific conditions need to be satisfied in order to store the optimum level of energy. The wireless power transmission (WPT) technique has been considered another alternative, thanks to the following advantages: 1) a larger amount of power can be supplied and 2) whenever it is required, power can be transferred to the wireless sensors.

In recent years, Kurs et al. [9] proposed a WPT technique using magnetic resonance. Compared to the well-known inductive coupling-based WPT [10, 11], this technique is

Manuscript received January 26, 2015 ; Revised February 23, 2015 ; Accepted March 11, 2015. (ID No. 20150126-003J)
[1]Department of Civil and Environmental Engineering, KAIST, Daejeon, Korea.
[2]Center for Integrated Smart Sensors, KAIST, Daejeon, Korea.
[*]Corresponding Author: Minseok Han (e-mail: mshan1024@kaist.ac.kr)

advantageous to transfer power without sharp degradation of power transmission efficiency (PTE) despite of the increase of transmission distance. Many related studies have been undertaken to increase transmission distance and efficiency through air [12−17]. Jonah and Georgakopoulos [18] examined PTE through concrete and reinforced concrete (i.e., concrete with rebars), which are inhomogeneous mediums. While the study of PTE change induced by thickness and humidity variations in concrete was successful, the analysis of concrete and steel rebar effects on PTE is still insufficient.

In this study, the magnetic resonance-based WPT (MR-WPT) technique is investigated. Resonance coils of 6.78 MHz are optimally designed to achieve a high Q-factor, and coil-to-coil PTE is experimentally measured and compared for three different mediums: air, unreinforced concrete, and reinforced concrete. The effects of concrete and steel rebars are analyzed in terms of PTE change.

In Section II, we explain the fundamental principles of MR-WPT, and in Section III, we describe resonance coil design procedures. The PTE of the designed resonance coils is evaluated and compared for different mediums in Section IV. A brief summary and suggestions for future work make up Section V.

II. Magnetic Resonance-based Wireless Power Transmission

MR-WPT is a mid-range WPT technique aiming to achieve power transmission distance of more than hundreds of millimeters.

Fig. 1 is a simplified circuit model of MR-WPT consisting of the transmitting (Tx) coil, the receiving (Rx) coil, a power source, and load. Two resonance coils of the same resonance frequency are coupled through a magnetic field that lies between them Fig. and power is transferred from the power source to the load through the magnetic field [18−20]. The coupling coefficient (k_{12}) between the resonance coils can be expressed as follows:

$$k_{12} = \frac{M_{12}}{\sqrt{L_1 L_2}}. \tag{1}$$

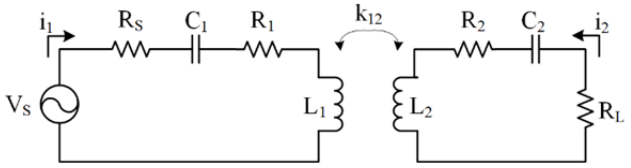

Fig. 1. A circuit model of magnetic resonance-based wireless power transmission: the transmitter and receiver circuits are described left and right, respectively, and the transmitting coil (L_1) and receiving coil (L_2) are magnetically coupled with a coupling coefficient of k_{12}.

L_1, L_2, and M_{12} are the self-inductance of each coil and mutual inductance, respectively. k_{12} represents the strength of magnetic coupling between the Tx and Rx resonance coils.

$$\begin{bmatrix} V_S \\ 0 \end{bmatrix} = \begin{bmatrix} Z_1 & j\omega M_{12} \\ j\omega M_{12} & Z_2 \end{bmatrix} \begin{bmatrix} i_1 \\ i_2 \end{bmatrix} \tag{2}$$

Eq. (2) is a node equation of the circuit model in Fig. 1. V_S is input voltage from the power source and ω is the designated resonance frequency of the coils. i_1 and i_2 denote the current of the transmitter and the receiver, respectively. Z_1 and Z_2 are the impedance of each circuit and can be calculated by Eq. (3):

$$\begin{aligned} Z_1 &= R_S + R_1 + j\left(\omega L_1 - \frac{1}{\omega C_1}\right), \\ Z_2 &= R_L + R_2 + j\left(\omega L_2 - \frac{1}{\omega C_2}\right). \end{aligned} \tag{3}$$

R_1, R_2, R_S, and R_L are the resistances of the Tx coil, the Rx coil, the power source, and the load, respectively. C_1 and C_2 represent the capacitance of the Tx and Rx coils.

After solving Eqs. (2) and (3) against i_2, load voltage, V_L, is computed as follows in Eq. (4):

$$V_L = -i_2 \cdot R_L = \left(\frac{V_S \cdot (j\omega M_{12})}{Z_1 Z_2 + \omega^2 M_{12}^2}\right) \cdot R_L. \tag{4}$$

When the system is supposed as a simple two-port network, the amount of transmitted power can be quantified using the *S*-parameter [18, 20]. As shown in Eq. (5), S_{21} can be acquired using the electric components of the circuit model, and the PTE (η) of the proposed MR-WPT is produced by Eq. (6):

$$S_{21} = 2\frac{V_L}{V_S}\left(\frac{R_S}{R_L}\right)^{1/2} \tag{5}$$

$$\eta = |S_{21}|^2 / (1 - |S_{11}|^2) \times 100\ (\%). \tag{6}$$

III. Design of Resonance Coils

The design of the resonance coils is one of the most significant procedures to maximize PTE.

$$Q = \frac{\omega L}{R} \tag{7}$$

Q is a calculated Q-factor of a coil and ω is a resonance frequency. L and R denote self-inductance and resistance of the coil, respectively. Because the PTE of the system (η) is directly related with its Q-factor, it is essential to realize a maximum Q-factor under the same geometric restrictions;

the relationship between them is provided in Eq. (8).

$$\eta = \frac{1}{1+\frac{1}{k_{12}^2 Q_1 Q_2}} \cdot \frac{R_L}{R_2+R_L} \tag{8}$$

Q_1 and Q_2 are Q-factors of the Tx and Rx coil, respectively, and k_{12} is the coupling coefficient between them. The R_2 denotes resistance of the Rx coil and R_L means load resistance.

In this study, a printed spiral form is employed to assure system stability against external impact, and an analytical approach to design the printed spiral coil for WPT is used, which was proposed by Jow and Ghovanloo [21]. Its resonance frequency is tuned to 6.78 MHz, which is designated as the standard frequency for WPT by the Alliance for Wireless Power (A4WP) [22].

Several geometric restrictions are decided 1) coil size is fixed to 300 × 300 mm^2 after considering convenience in practical uses, and 2) copper thickness and the spacing between copper lines are limited to 0.1 mm and 0.6 mm, respectively, because of technical limitations in manufacturing. Multiple design sets are produced in certain ranges, followed by previously determined geometric restrictions. The self-inductance, parasitic capacitance, and Q-factor of each design set are computed to determine optimum design parameters. For example, the number of turns from 4 turns to 15 turns, copper width from 1 mm to 10 mm, and spacing from 0.6 mm to 2.0 mm are assigned as the range of design parameters. Out of the computed design sets, one is picked that satisfies the following two conditions: 1) resonance frequency is between 6.78 MHz and 7.45 MHz and 2) the highest Q-factor is produced out of the design sets in condition (1).

Table 1 shows the determined design parameters and electric specifications of each computed and fabricated resonance coil. Computed design parameters are well matched with the fabricated ones, meaning that the optimization process using the analytical approach is successful. Fig. 2 is the fabricated resonance coil according to the design parameters determined by previously mentioned procedures. Thanks to the stiffness of the printing substrate, the stability of the MR-WPT system is assured during the experiment.

Table 1. Design parameters and electric specifications of each computed and fabricated resonance coil

	Computed resonance coil	Fabricated resonance coil
Number of turns	11 turns	
Copper width	7 mm	
Spacing	0.6 mm	
Copper thickness	0.1 mm	
Self-inductance	32.16 μH	31.54 μH
Resistance	5.35 Ω	5.21 Ω
Parasitic capacitance	16.97 pF	17.01 pF
Q-factor	256.06	242.69

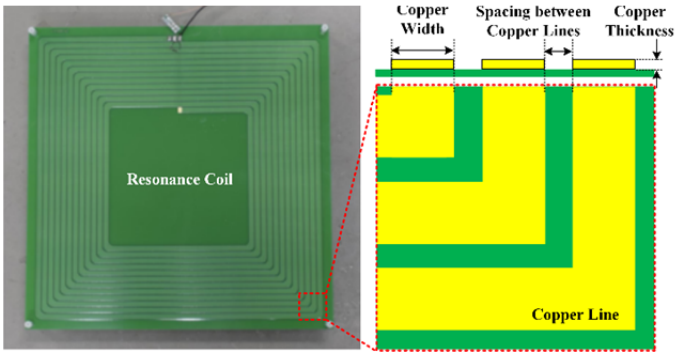

Fig. 2. Fabricated resonance coil with brief description of design parameters: the resonance coil is fabricated as a printed spiral type and FR-4 is used as a substrate.

Table 2. Mix proportioning for concrete structures

Gradient	Unit weight (kg/m^3)
Cement	480
Water	164
Sand	778
Gravel	869
WRA	58.9

Table 3. Geometric information about concrete structures

Geometric information	Value
Concrete size ($W \times H \times T$)	600 × 600 × 300 mm^3
Diameter of steel rebar	15 mm
Spacing of steel rebar	150 mm

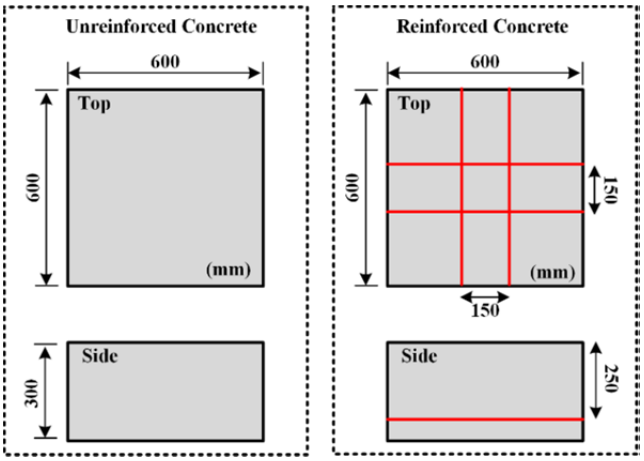

Fig. 3. Blueprints of unreinforced and reinforced concrete. The same mix proportioning is used for both unreinforced and reinforced concretes and the diameter of the used steel rebars is set at 15 mm.

IV. Experimental Validations

In Section IV, the PTE of the designed resonance coils is experimentally measured for three different mediums: air, unreinforced concrete, and reinforced concrete. By observing the PTE changes of each condition, the effects of concrete and steel rebars on PTE are analyzed.

Two concrete structures are specially designed. One is unreinforced concrete and the other is reinforced concrete using steel rebars, the diameter of which is 15 mm. The mix proportioning and detailed geometric information are shown in Tables 2 and 3. In particular, not only the concrete thickness and the spacing of steel rebars but also the compressive strength are carefully determined while considering real concrete bridge construction. Blueprints for the manufactured concrete structures are shown in Fig. 3. Concrete size is 600 $\times$600 $\times$300 mm^3, and steel rebars are placed at a 50-mm distance from the bottom.

Experimental setups for PTE measurement using MR-WPT through air and concrete structures are shown in Fig. 4. For both conditions, Tx and Rx coils are placed at the top and bottom, respectively, and the distance between them is fixed at 330 mm. In particular, Tx and Rx coils are 15 mm distant from the top and bottom surfaces of the concrete structure.

The reflection coefficients (S_{11}, S_{22}) at the Tx and Rx coils

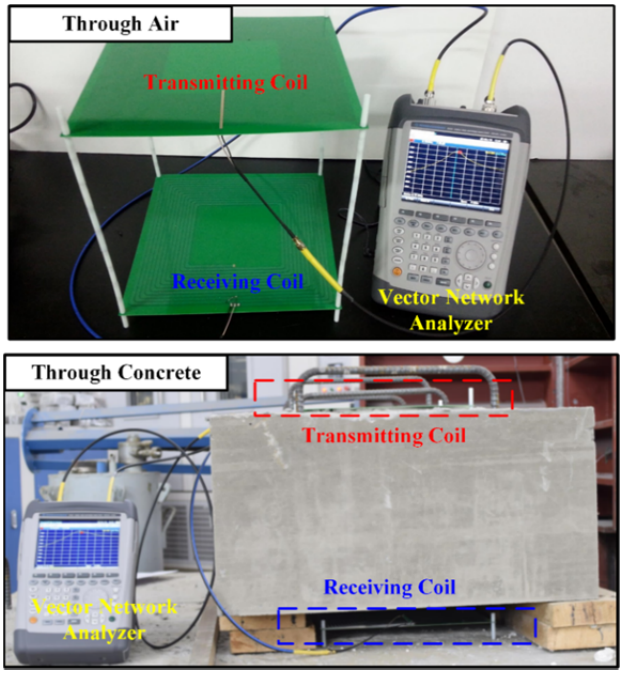

Fig. 4. Experimental setups for power transmission efficiency (PTE) measurement using magnetic resonance-based wireless power transmission through air and concrete structures. The distance between two coils is set to be equal for both experiments at 330 mm, and the PTE is measured using a vector network analyzer.

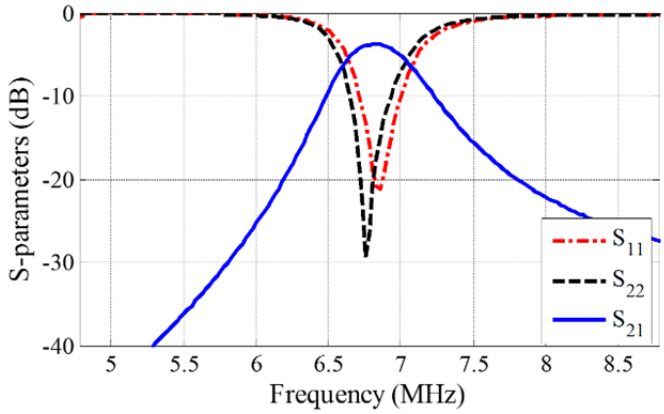

Fig. 5. Measured S-parameter characteristics through air: S_{11}, S_{22}, and S_{21} at 6.78 MHz are measured as -15.92 dB, -26.36 dB, and -3.86 dB, respectively.

Table 4. Measured coupling coefficient (k) and mutual inductance (M) for each case

	Coupling coefficient	Mutual inductance(μH)
Air	0.0267	0.89
Unreinforced concrete	0.0288	0.96
Reinforced concrete	0.0281	0.93

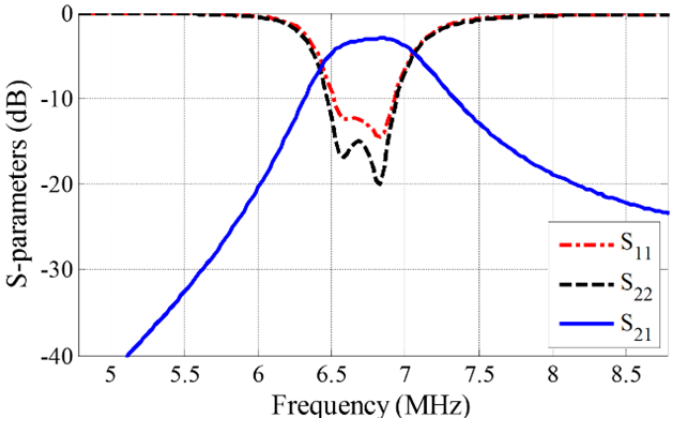

Fig. 6. Measured S-parameter characteristics through unreinforced concrete: S_{11}, S_{22}, and S_{21} at 6.78 MHz are measured as -13.66 dB, -18.07 dB, and -3.02 dB, respectively.

and the transmission coefficient (S_{21}) are measured and the results are shown in Figs. 5–7. While S_{11} and S_{22} clearly have a single peak in the air condition, the frequency splitting phenomena happens when concrete is placed close to Tx and Rx coils. Comparing the PTE of each condition in Fig. 8, the existence of concrete increases and stabilizes the PTE over a broader frequency range than the air condition. Despite the expected reflections and attenuations of electromagnetic waves caused by the concrete structure, concrete brings about an improvement in PTE compared to the air condition. The reason might be that the included cement is paramagnetic

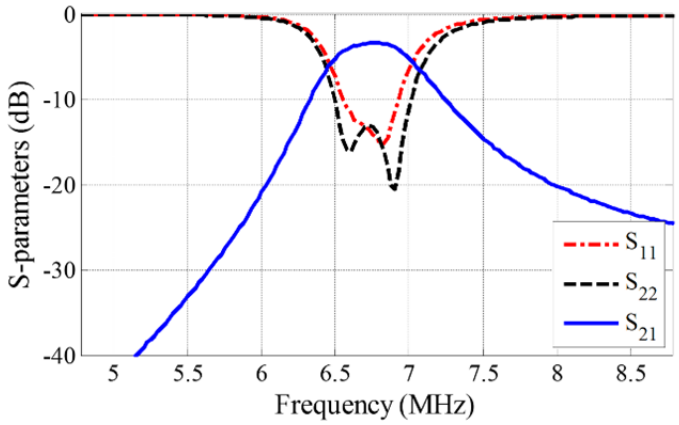

Fig. 7. Measured *S*-parameter characteristics through reinforced concrete: S_{11}, S_{22}, and S_{21} at 6.78 MHz are measured as −14.54 dB, −13.91 dB, and −3.43 dB, respectively.

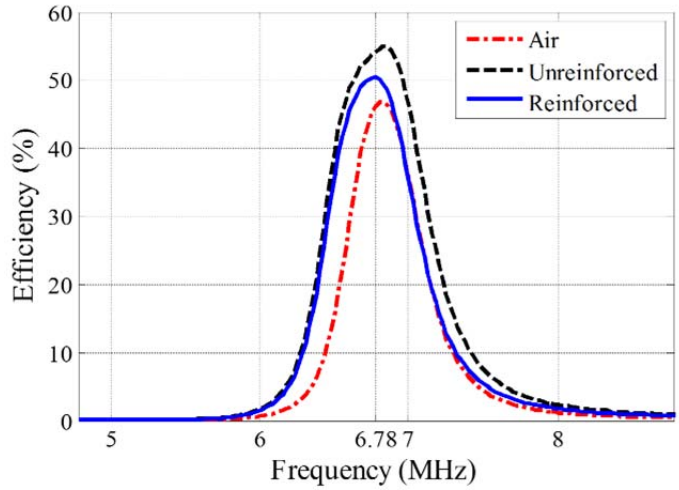

Fig. 8. Transmission efficiency for different mediums: power transmission efficiency through air, unreinforced concrete, and reinforced concrete are measured as 46%, 54%, and 51%, respectively.

(magnetic susceptibility > 0) [23] and the degree of this effect depends on the dielectric properties determined by mix proportioning. The coupling coefficient (k) and mutual inductance (M) for each case are measured and are given in Table 4.

On the other hand, steel rebars, which are conductors, definitely cause degradation of the PTE because of the reflections and eddy currents induced by alternating the magnetic field on their surfaces. In fact, the PTE of reinforced concrete is approximately 3% lower than that of unreinforced concrete, according to the experimental results.

V. Conclusion

In this study, an MR-WPT system was developed and the effects of concrete and steel rebars on PTE were examined using the developed system. The resonance coil with 6.78 MHz frequency was analytically designed to produce a maximum Q-factor. Unreinforced and reinforced concrete were specially designed following the construction conditions of real concrete bridges. PTE was measured and compared for three different mediums: air, unreinforced concrete, and reinforced concrete. Despite the expected reflections and attenuations of electromagnetic waves caused by the concrete structure, the existence of concrete induces improvements in the PTE. Concrete affects the generation of a magnetic field between resonance coils, and the detailed interactions are worth investigating numerically and analytically in future research. Comparing the results of unreinforced and reinforced concrete, it is proved that steel rebars of 150 mm spacing cause approximately a 3% degradation in PTE.

This study showed that MR-WPT is a promising technique to power wireless sensors in SHM for reinforced concrete structures. In the future, independent MR-WPT systems will be developed, including amplifying and rectifying circuits and the application to power wireless sensors. Finally, the applicability of the developed MR-WPT system for in-service reinforced concrete structures will be experimentally validated.

This study is supported by a grant from Smart Civil Infrastructure Research Program (No. 13SCIPA01) funded by Ministry of Land, Infrastructure and Transport (MOLIT) of Korea government and the Center for Integrated Smart Sensors funded by the Ministry of Science, ICT & Future Planning as Global Frontier Project (No. CISS-2012M3A6A6054193).

References

[1] H. J. Lim, H. Sohn, and P. Liu, "Binding conditions for nonlinear ultrasonic generation unifying wave propagation and vibration," *Applied Physics Letters*, vol. 104, no. 21, article no. 214103, 2014.

[2] A. Sophian, G. Y. Tian, and S. Zairi, "Pulsed magnetic flux leakage techniques for crack detection and characterization," *Sensors and Actuators A: Physical*, vol. 125, no. 2, pp. 186−191, 2006.

[3] S. Wagle and H. Kato, "Ultrasonic detection of fretting fatigue damage at bolt joints of aluminum alloy plates," *International Journal of Fatigue*, vol. 31, no. 8, pp. 1378−1385, 2009.

[4] S. J. Cho, H. Jo, S. Jang, J. W. Park, H. J. Jung, C. B. Yun, B. F. Spencer, and J. W. Seo, "Structural health monitoring of a cable-stayed bridge using wireless smart sensor technology: data analyses," *Smart Structures and Systems*, vol. 6, no. 5−6, pp. 461−480, 2010.

[5] S. N. Pakzad, G. L. Fenves, S. Kim, and D. E. Culler, "Design and implementation of scalable wireless sensor network for structural monitoring," *Journal of Infrastructure Systems*, vol. 14, no. 1, pp. 89−101, 2008.

[6] H. J. Jung, I. H. Kim, and S. J. Jang, "An energy harvesting system using the wind-induced vibration of a stay cable for powering a wireless sensor node," *Smart Materials and Structures*, vol. 20, no. 7, article no. 075001, 2011.

[7] H. Kulah and K. Najafi, "Energy scavenging from low-frequency vibrations by using frequency up-conversion for wireless sensor applications," *IEEE Sensors Journal*, vol. 8, no. 3, pp. 261−268, 2008.

[8] C. R. Saha, T. O'donnell, N. Wang, and P. McCloskey, "Electromagnetic generator for harvesting energy from human motion," *Sensors and Actuators A: Physical*, vol. 147, no. 1, pp. 248−253, 2008.

[9] A. Kurs, A. Karalis, R. Moffatt, J. D. Joannopoulos, P. Fisher, and M. Soljačić, "Wireless power transfer via strongly coupled magnetic resonances, " *Science*, vol. 317, no. 5834, pp. 83−86, 2007.

[10] J. Sallán, J. L. Villa, A. Llombart, and J. F. Sanz, "Optimal design of ICPT systems applied to electric vehicle battery charge," *IEEE Transactions on Industrial Electronics*, vol. 56, no. 6, pp. 2140−2149, 2009.

[11] Z. N. Low, R. A. Chinga, R. Tseng, and J. Lin, "Design and test of a high-power high-efficiency loosely coupled planar wireless power transfer system," *IEEE Transactions on Industrial Electronics*, vol. 56, no. 5, pp. 1801−1812, 2009.

[12] A. Kurs, R. Moffatt, and M. Soljačić, "Simultaneous mid-range power transfer to multiple devices," *Applied Physics Letters*, vol. 96, no. 4, article no. 044102, 2010.

[13] J. Kim, H. C. Son, K. H. Kim, and Y. J. Park, "Efficiency analysis of magnetic resonance wireless power transfer with intermediate resonant coil," *IEEE Antennas and Wireless Propagation Letters*, vol. 10, pp. 389−392, 2011.

[14] J. M. Kim, M. S. Han, and H. Sohn, "Wireless power transmission through concrete using magnetically-coupled resonators," in *Proceedings of the 10th International Workshop on Advanced Smart Materials and Smart Structures Technology (ANCRiSST 2014)*, Taipei, Taiwan, 2014, pp. 65−66.

[15] B. C. Park, Y. H. Son, B. J. Jang, and J. H. Lee, "Realization of alignment-free WPT system," *Journal of Electromagnetic Engineering and Science*, vol. 14, no. 4, pp. 329−331, 2014.

[16] T. Oh and B. Lee, "Analysis of wireless power transfer using metamaterial slabs made of ring resonators at 13.56 MHz," *Journal of Electromagnetic Engineering and Science*, vol. 13, no. 4, pp. 259−262, 2013.

[17] J. H. Kim, B. C. Park, and J. H. Lee, "New analysis method for wireless power transfer system with multiple n resonators," *Journal of Electromagnetic Engineering and Science*, vol. 13, no. 3, pp. 173−177, 2013.

[18] O. Jonah and S. V. Georgakopoulos, "Wireless power transfer in concrete via strongly coupled magnetic resonance," *IEEE Transactions on Antennas and Propagation*, vol. 61, no. 3, pp. 1378−1384, 2013.

[19] S. Cheon, Y. H. Kim, S. Y. Kang, M. L. Lee, J. M. Lee, and T. Zyung, "Circuit-model-based analysis of a wireless energy-transfer system via coupled magnetic resonances," *IEEE Transactions on Industrial Electronics*, vol. 58, no. 7, pp. 2906−2914, 2011.

[20] H. Hoang and F. Bien, "Maximizing efficiency of electromagnetic resonance wireless power transmission systems with adaptive circuits," in *Wireless Power Transfer: Principles and Engineering Explorations*, K. Y. Kim, Ed. Rijeka, Croatia: InTech, 2012.

[21] U. M. Jow and M. Ghovanloo, "Design and optimization of printed spiral coils for efficient transcutaneous inductive power transmission," *IEEE Transactions on Biomedical Circuits and Systems*, vol. 1, no. 3, pp. 193-202, 2007.

[22] *A4WP Wireless Power Transfer System Baseline System Specification (BSS) v.1.2*, The Alliance for Wireless Power (A4WP), 2014.

[23] R. Gopalakrishnan, S. Barathan, and D. Govindarajan, "Magnetic susceptibility measurements on fly ash admixtured cement hydrated with groundwater and seawater," *American Journal of Materials Science*, vol. 2, no. 1, pp. 32−36, 2012.

Ji-Min Kim

received his B.S. degree from Korea Advanced Institute of Science and Technology (KAIST), Daejeon, South Korea in 2012, where he is currently working toward Ph.D. degree in civil and environmental engineering. His research interests include nondestructive testing, structural health monitoring using wireless sensors and wireless power transmission through magnetic resonance.

Minseok Han

received a B.S. in Electrical Engineering from Ajou University, Suwon, Korea, in 2002. He received his M.S. and a Ph.D. from the Division of Electrical and Computer Engineering at Hanyang University, Seoul, Korea, in 2005 and 2011, respectively. From 2005 to 2007, he worked with the LG Electronics Institute of Technology, where he has been engaged in the design of multi-band internal antenna for mobile handsets. He worked with LS Cable & System as a chief research engineer in the Communication Solution Division from 2011 to 2013. Since 2013, he has been a research professor in the Center for Integrated Smart Sensors, Korea Advanced Institute of Science and Technology (KAIST), Korea. His research interests include antennas, RF devices, and wireless power transfer systems. Currently, his researches are mainly focused on wireless power transfer systems for various consumer electronics, wireless sensor networks and smart mobility applications.

Hoon Sohn

received his B.S. and M.S. degree from Seoul National University, Seoul, South Kora in 1992 and 1994, respectively, and Ph.D. degree from Stanford University, CA, USA in 1998. From 2001 to 2004, he worked at Los Alamos National Laboratory, NM, USA as technical staff member. He joined to Carnegie Mellon University, PA, USA as assistant professor from 2004 to 2006. He is currently chaired professor in civil and environmental engineering in Korea Advanced Institute of Science and Technology (KAIST) from 2007 to present. His research interests includes nondestructive testing, structural health monitoring, noncontact sensing technologies, smart materials & structures, statistical pattern recognition and signal processing.